High-Voltage and High-Amperage Current Pulse Generator for Experimental Magnetic Therapy

Pavel Hanak, Kamil Vrba

***Abstract*—**This paper presents a high-amperage current pulse generator with a high-voltage internal power supply. The generator was designed and constructed specifically for upcoming magnetic therapy experiments on cancerous tissues and can deliver currents up to ±100A. The high-voltage power supply will be needed to achieve fast current changes in the large application coils. Due to the high required currents, the generator uses a relatively simple switching-mode approach and employs full bridge of power IGBT transistor as the switches. This has the advantage of very high power efficiency, but the output waveforms are limited to short current spikes only.

***Keywords*—**Magnetic therapy, cancer, toroidal coil, current pulse generator, electric field, power transistor bridge.

I. Introduction

EFFECTS of time-varying electromagnetic fields on living tissues have been known for a long time and are employed in clinical practice for at least 40 years. There exist several monographs about the subject, for example [1], [2]. Such applications of electromagnetic fields on living subjects are colloquially called "magnetic therapy", although in many cases this is technically incorrect.

Our team performs research into effects of various electromagnetic fields on tumor tissues. Due to speculative nature of the research, experiments on various human carcinoma lines are performed only in-vitro [3]. However, we have also performed some in-vivo experiments with live tumors in animal models, most notably on laboratory rats of the Lewis line. Setup for one such experiment is in figure 1. In this case, a rat was artificially implanted with sarcoma cells of the R5-28-7 line; the cells were then allowed to grow into a large tumor. The rat was then placed inside two closely spaced toroidal ferrite coils whose outer diameter was 152 mm. The rat was under general anesthesia and lied on plastic slider, which allowed precise positioning of the tumor along the application coils' axis.

Manuscript received November 8, 2010. This work was supported by the Ministry of Education, Youth and Sports of the Czech Republic under Grant No. 2B08063 and under Grant No. 3025/2010/F1a.

Pavel Hanak, MSc. is with the Brno University of Technology, Department of Telecommunications, Brno, Czech Republic (phone: +420 541149252; e-mail: hanakp@feec.vutbr.cz).

Kamil Vrba, Prof., Ph.D. is with the Brno University of Technology, Department of Telecommunications, Brno, Czech Republic (phone: +420 541149189; e-mail: vrbak@feec.vutbr.cz).

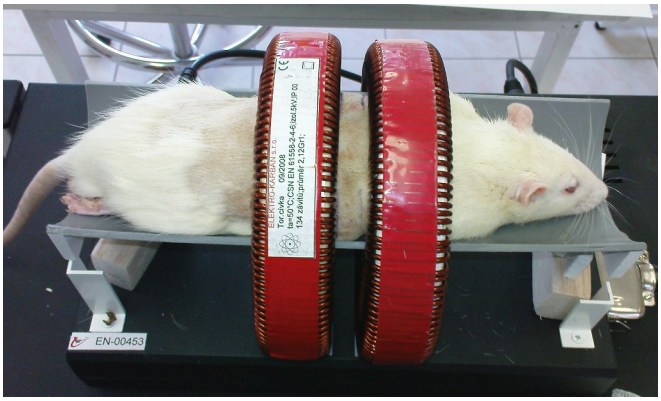

Fig. 1. Cancerous Lewis rat inside two toroidal coils

This experimental setup was not chosen randomly. In the past, we have performed computer simulations of various combinations of toroidal coils in order to determine the shapes and intensities of the generated fields; the simulations were done in ANSYS. Results of some earlier simulations were presented in [4].

Example of one such simulation is in figure 2, which depicts generated electric field **E** of four co-axial toroidal coils which were excited by anti-phase currents. Figure depicts one-quarter slice of the coils and associated field intensities are represented by a color map. The result shows that the spatial electric field intensity on the coils' common axis is greater than 3400 Vm^{-1} (±1700 Vm^{-1}). Such result is very interesting, because it has been proven that electric fields of certain frequencies can significantly slow down the growth rate of some types of malignant tumors [5].

Unfortunately, the intensity of the generated electric field is dependent on the time rate of change of the current flowing through the coils, as can be derived from Maxwell's equations

$$\mathbf{E} = -\nabla\phi - \frac{\partial \mathbf{A}}{\partial t}, \qquad (1)$$

where **A** is the magnetic vector potential, which itself is directly related to the current flowing through the coil. To obtain high electric fields, it is necessary to change the current rapidly. This fact presents an engineering problem, because

ISBN: 978-960-474-250-9

every coil naturally resists any changes of its current. This is mathematically expressed

$$u_{\mathrm{L}}(t) = L(i_{\mathrm{L}})\frac{\mathrm{d}i_{\mathrm{L}}(t)}{\mathrm{d}t}, \tag{2}$$

or by simplified equation for the case of a linear inductor

$$\Delta u_{\mathrm{L}} = L\frac{\Delta i_{\mathrm{L}}}{\Delta t}. \tag{3}$$

As is apparent from (3), there are only two ways of quickly forcing a current change into an inductor: either by reducing its inductance L or by increasing voltage swing Δu_{L}. Therefore, any current generator used to force the current through the coils should have a high-voltage internal power supply.

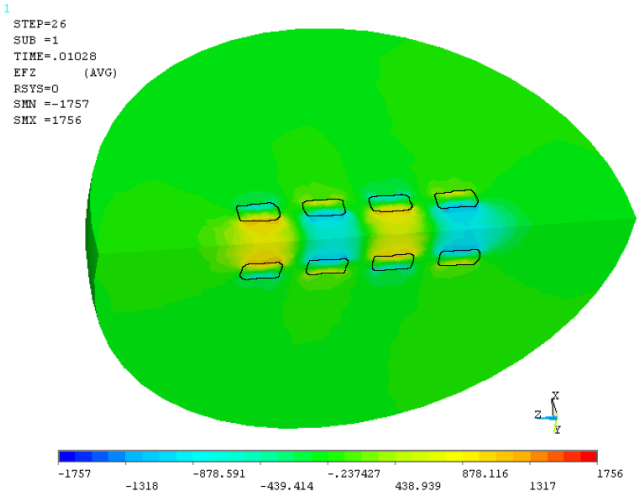

Fig. 2. ANSYS simulation of four co-axial toroidal coils

Our team has developed a high-amperage generator for magnetic therapy experiments before [6]. It used a 60 V internal power supply and its parameters were sufficient for most experiments. But in the future, we will need to confirm our results from the rat models on other animal tumors. One of our co-researchers, Institute of Animal Physiology and Genetics of the Czech Republic, breeds laboratory miniature pigs of the MeLiM line [7]. These pigs have been selective bred with the aim to induce strong congenital predispositions for malignant melanoma and other cancer types. We are currently working on an experimental setup with two massive toroidal coils with 600 mm outer diameter, which should be able to accommodate these pigs. Such large coils of course have big inductance and the old generator [6] is unable to force current though them quickly enough. Therefore, we have constructed a new, approximately 10 times faster generator, which is described in this paper. The generator was given designation H02.

II. Current Pulse Generator H02

A. Design parameters

As was explained above, the electric field is generated only when current thought the application coils changes. Therefore, the generator should be able to generate short current pulses with fast rise and fall times. Since we are interested only in current change, the pulses can have shape of mere narrow spikes, as depicted in figure 3. For flexibility during the experiments, positive, negative and bipolar pulse generation modes were implemented into the generator.

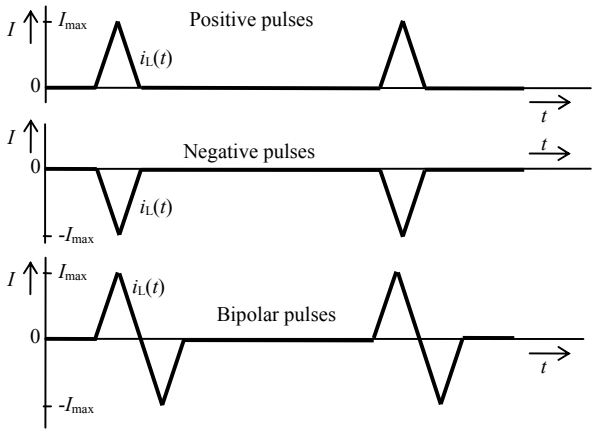

Fig. 3. Requested output current pulse waveforms

Due to large physical dimensions of the future coils, the generator H02 was designed for relatively high maximum output current amplitudes of ±100 A. To achieve high current change in the coils, the generator has to use a high-voltage power source. H02 employs a 600 V safety power supply, which is 10 times higher voltage than its predecessor [6]. Because the actual biological experiments are performed by medical personnel with little or no education in electrotechnology, the generator had to be equipped with an intuitive user interface.

B. Block diagram

Block diagram of the H02 generator is in figure 4. Since only narrow spike-shaped current pulses were required, the generator was designed with switching-mode topology. The application coil L_A is connected into full transistor bridge. Such topology is well known in power electronics applications [8], but its function is different in the H02 generator, as will be explained in the next chapter. The bridge was built from two IGBT transistor modules [9] with nominal $I_C = 200$ A and $V_{CE} = 1200$ V.

The bridge is powered by a galvanically isolated (safety) power supply $V_B = 600$ V. The power supply employs traditional approach with 300 VA toroidal transformer, bridge rectifier and storage capacitor C_S. The storage capacitor is comprised of 8 individual, low ESR 47 mF/100 V capacitors connected in series; together, they form one 5.9 mF/800 V capacitor. Parasitic inductance of this capacitor is suppressed by two special 1.5 uF/1000 V inductance-less pulse foil

ISBN: 978-960-474-250-9

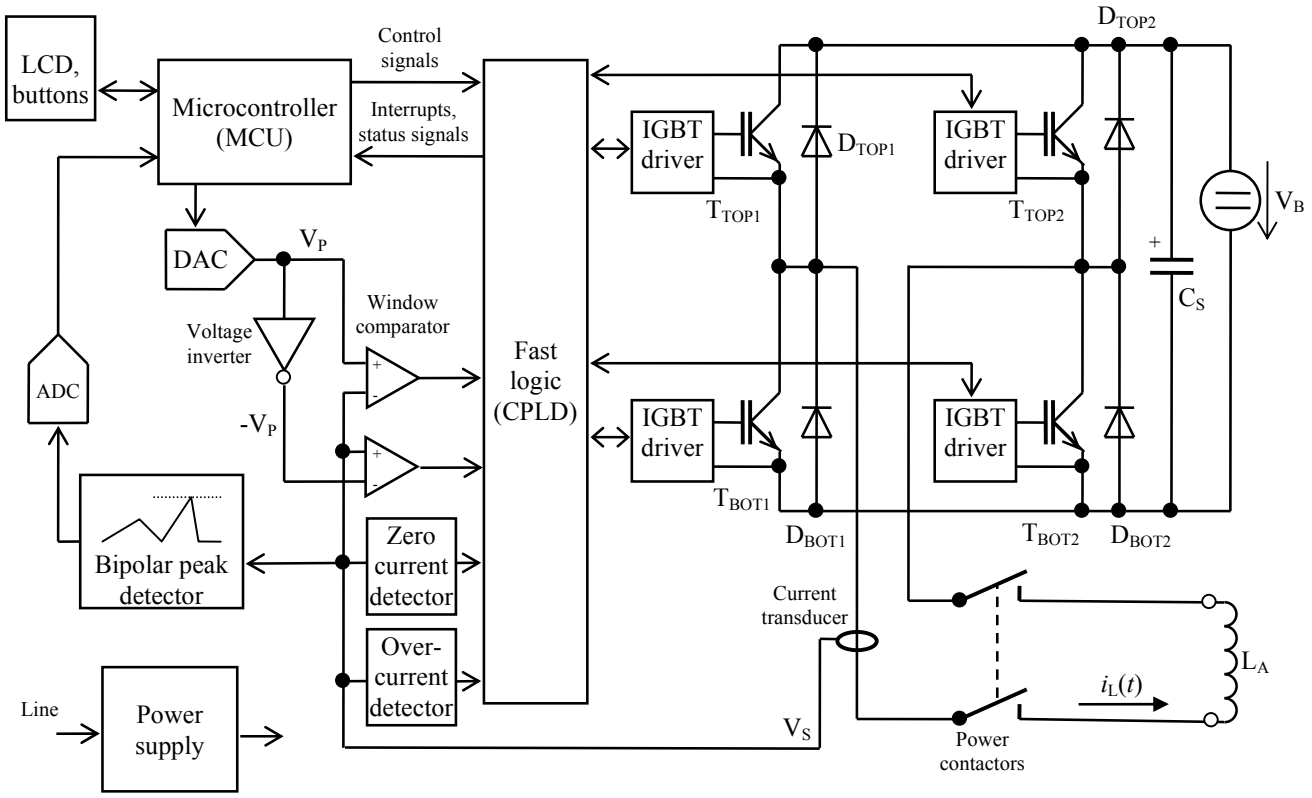

Fig.4. Block diagram of H02 current pulse generator

capacitors, which were mounted directly to both IGBT modules in the bridge. These capacitors suppress voltage overshoots which occur during turn-off events and can damage the transistors by excessive V_{CE} voltage.

The transistors are controlled by specialized IGBT drivers [10], which are manufactured specifically for this purpose. The drivers provide galvanic isolation between the high-voltage bridge and low-voltage controlling logic circuits. The entire transistor bridge is thus galvanically isolated from the rest of the generator, which enhances safety. The drivers contain hardware interlocks and protection which prevent transistor damage in case of a short circuit and/or severe overcurrent conditions in the bridge. The drivers report any switching faults back to the control circuits.

The applicator coil L_A is connected to the generator via massive, low-resistance screw clamps. In the idle state, these clamps are physically disconnected from the transistor bridge by power contactors. This was required due to safety regulations – a closed semiconductor switch cannot be considered as safety disconnecting device, especially when operating with hazardous voltage of 600 V. The contactors ensure that the user will not receive an electric shock during manipulation with the application coil.

The actual value of the current $i_L(t)$ though L_A is continuously monitored by an isolated current transducer [11] which provides linear voltage representation (signal V_S) of the flowing current. Voltage V_S is then used in a window comparator and in zero and overcurrent detectors.

The window comparator compares actual value of $i_L(t)$ (represented by V_S) with user-defined pulse amplitude I_P (represented by V_P from the DAC). The window comparator is necessary to be able to detect both current polarities (directions). The comparators are prone to oscillations in such switching applications. To suppress them, special comparators with embedded internal hysteresis were chosen [12].

The entire generator is controlled by an embedded microcontroller (MCU) which also provides a user interface with dot-matrix LCD display and four push-buttons. However, microcontrollers are generally too slow for switching applications. The main signal processing and control is therefore performed in the block of fast digital logic. To allow for greater design freedom, this control logic was realized with help of a complex programmable logic device (CPLD) [13]. The CPLD and MCU are tied together via several control and status signals and two interrupt request signals.

There were problems with overcurrent spikes when some nonlinear coils were connected the old generator [6]. The overcurrents were significant; they could be as high as 130% of the desired current amplitude. This was caused mainly by various propagation delays in the signal path between the window comparator and the IGBT transistors. Of these delays, the most significant were those introduced by the IGBT drivers (1,4 µs) and the turn-off delay of the transistors themselves (0,7 µs). Simply put, the current through the coil still rose for at least 2,1 µs even when the comparator already signaled that it should stop. Therefore, the H02 generator

ISBN: 978-960-474-250-9

contains a bipolar peak detector and ADC, which measures the real amplitude of the generated pulses. The microcontroller contains a software feedback loop, which compares the actual measured value with the desired amplitude and makes appropriate corrections to the V_P control voltage. This way, the effects of the delays are compensated. This solution has the advantage that it is adaptive; the software feedback will always ensure the correct current amplitude, regardless of the application coil's inductance or ferromagnetic core type. The peak detector is based on a known circuit topology [14] and employs fast rail-to-rail operational amplifiers [15].

C. Pulse generation sequence

The function of the entire generator will be explained on the case of positive current pulses. For better understanding, it is appropriate to split the pulse's waveform into a few individual phases as depicted in figure 5. Before pulse generation starts, the microcontroller has to reset the any random signals, which can occur in CPLD, IGBT drivers etc. after power-up. Next, the DAC is set so its output voltage V_P corresponds to the required pulse amplitude I_P.

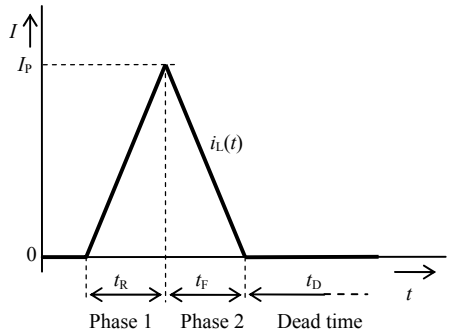

Fig. 5. Positive pulse generation phases

Phase 1 (rising edge) begins when MCU switches on transistors T_{TOP1} and T_{BOT2}. This effectively connects L_A to the voltage V_B and the current $i_L(t)$ in the inductor begins to rise until it reaches predefined amplitude $+I_P$. At this point, voltage V_S from the current transducer becomes equal to the voltage V_P from the DAC and the window comparator flips. Signal from the comparator is evaluated in the CPLD and both transistors are quickly switched off. Thus begins the Phase 2. Because the inductor L_A attempts to preserve the direction of the current flowing though it, it now acts as a power source and voltage on its terminals reverses. This voltage opens diodes D_{BOT1} and D_{TOP2} and the inductor L_A begins to demagnetize itself back into the storage capacitor C_S until current $i_L(t)$ reaches zero. Such condition is detected by the zero current detector and the CPLD invokes another interrupt to notify the MCU. After predefined dead time t_D between individual pulses, the MCU incites new Phase 1 and another pulse is generated. Note that in the case of linear inductor L_A, the rise and fall times (t_R and t_F in figure 5) can be roughly calculated using (3).

The negative pulse generation sequence is similar, but uses transistors T_{TOP2} and T_{BOT1} instead. Bipolar pulse generation begins as in the case of positive pulse, but when the current reaches the $+I_P$, the T_{TOP1} and T_{BOT2} transistors are turned off and T_{TOP2} and T_{BOT1} are turned on. The current is then allowed swing through zero to the $-I_P$ value. When this happens, the T_{TOP2} and T_{BOT1} transistors are switched off and L_A is allowed to demagnetize itself into the storage capacitor C_S until $i_L(t)$ reaches zero.

D. User interface

The user interface employs a backlit, 16x2 character dot-matrix LCD display and four push-buttons which were named Parameter, Up, Down and Start/Stop. The generator can switch between two main modes, Settings mode and Running mode. After power-up, the generator is always in Settings mode. In this mode, the pulse generation is blocked and user can change properties of the current pulses to be generated. The Parameter button cycles between individual parameters, their value can be changed using Up and Down buttons. List of all parameters that can be changed by user and their ranges can be found in table I. When the user is satisfied with all parameters, button Start/Stop can be used to start up actual generation of the current pulses (Running mode). The pulses will be generated until predefined Application time t_A runs out, or generator detects some kind of hardware of software error. The user can also stop the Running mode prematurely by pressing the Start/Stop button again. In any case, the generator will report (on the LCD) what stopped the Running mode and then will return to the Settings mode automatically.

TABLE I. USER-DEFINABLE PULSE PARAMETERS

Parameter	Symbol	Min value	Max value	Step
Pulse amplitude	I_P [A]	5	100	5
Dead time	t_D [ms]	1	200	1
Application time	t_A [min]	1	60	1
Pulse mode	Positive, negative or bipolar			

III. PHYSICAL REALISATION AND MEASUREMENTS

The H02 pulse generator was built into a rugged aluminum case with 560 x 560 x 110 mm outer dimensions. Its front panel and internal arrangement is apparent from figures 6 and 7, respectively. The finished instrument weighs 28 kg.

Fig. 6. Front view of H02 generator

As is apparent from figure 7, all control circuits are placed on a single circuit board with the exception of LCD and pushbuttons, which are mounted on a small separate board behind the front panel. Small power supplies for control electronics are placed on another auxiliary board near the toroidal transformer. This board moreover contains rectifier for the 600 V power supply and safety charging and discharging circuits for the C_S capacitor.

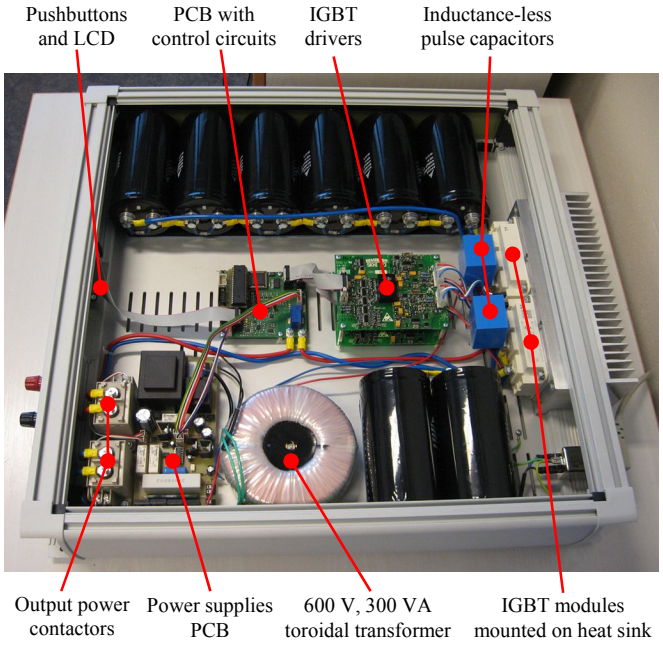

Fig. 7. Top view inside the generator

Internal power connections between the C_S capacitor and IGBT modules were done by 6 mm^2 gauge copper wires. The wires are carefully placed (and twisted whenever possible) so that their generated magnetic fields cancel each out. This prevents coupling of unwanted noise into the control circuits.

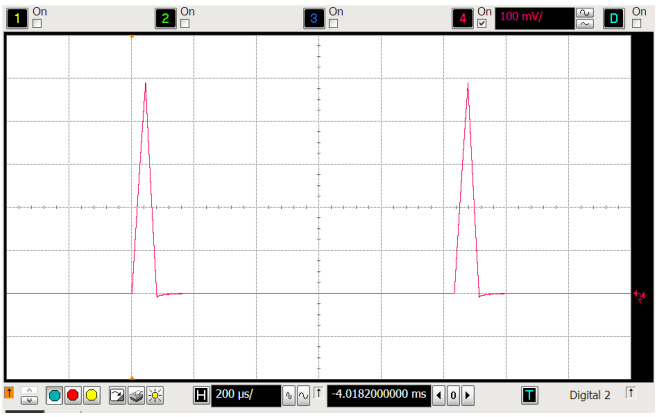

Fig. 8. Measured output current waveform, I_P = 25 A, t_D = 1 ms

The control circuits were broken up into three separate ground planes – analog, digital and power driver. All three grounds are connected together in one point only and this point connects them with earth potential. This ground topology was necessary to prevent noise injection from fast switching circuits into the analog parts, especially the comparators. Thanks to these precautions, the sensitive control circuits require no additional shielding against the electromagnetic interference.

Current waveforms produced by the finished instrument were measured with the help of a Tektronix TCP303 current probe; the probe was set to 50 A/V range. Figure 8 depicts measured positive pulses with amplitude of 25 A and 1 ms dead time between them; linear (air-core) inductor with inductance of 1 mH was used as the generator's load. Vertical sensitivity in figure 8 is 100 mV/div and time base is 200 µs/div. Measured rise and fall times were approximately 26 µs, which is in good relation with theory (3).

Small undershoot is visible on the falling edge of the current pulse; it is caused by reverse recovery energy stored in the power diodes in the bridge.

References

[1] K. S. Cole. *Membranes, Ions and Impulses: A Chapter of Classical Biophysics.* University of California Press, Berkeley, 1968. ISBN 978-0520002517.

[2] F. S. Barnes, B. Greenebaum. *Handbook of Biological Effects of Electromagnetic Fields, Third Edition.* CRC Press, 2006. ISBN 978-0849329524.

[3] O. Stehlikova, M. Klabusay, L. Palko, I. Rampl. Influence of Impulse Vector Magnetic Potential (IVMP) on Tumor Cell Lines. *Proceedings of International Conference on Bioengineering and Bionanotechnology.* Rome, Italy, 2009. ISSN 2070-3724.

[4] P. Hanak, T. Bachorec, K. Vrba. Transient Simulation of Large Toroidal Coils for Use in High-Amperage Magnetic Therapy. *Proceedings of the 32nd International Conference on Telecommunications and Signal Processing.* Asszisztencia Szervezo Kft., Budapest, 2009. ISBN 978 963-06-7716-5.

[5] E. D. Kirson et al. Alternating electric fields arrest cell proliferation in animal tumor models and human brain tumors. *Proceedings of the National Academy of Sciences of the USA*. Vol. 104, no. 24, pp. 10152-10157. Washington DC, June 2007. ISSN 1091-6490.

[6] P. Hanak, K. Vrba, M. Kohoutek. Single-Output, High-Amperage Digitally Controlled Current Pulse Generator for Magnetic Therapy. *Proceedings of 31st Telecommunications and Signal Processing conference.* Asszisztencia Szervezo Kft, Budapest, 2008. ISBN 978-963-06-5487-6.

[7] V. Hruban et al. Inheritance of malignant melanoma in the MeLiM strain of miniature pigs. *Veterinary medicine*, vol. 49, pp. 453-459. Inst Agricultural food information, Prague, 2004. ISSN 0375-8427.

[8] V. K. Khanna, *Insulated Gate Bipolar Transistor IGBT Theory and Design*. San Francisco: Wiley-IEEE Press, 2003. ISBN 0471238457.

[9] Semikron SKM 200GB126D IGBT Power Transistor Module Datasheet. Semikron International GmbH, Nurnberg, 2009.

[10] Semikron SKHI 23/12 Medium Power Double IGBT Transistor Driver Datasheet. Semikron International GmbH, Nurnberg, 2006.

[11] LEM LA-100P Closed-Loop Hall Effect Isolated Current Transducer Datasheet. LEM SA, Geneva, 2006.

[12] Analog Devices ADCMP602 Very Fast Rail-to-Rail Comparators Datasheet. Analog Devices, Inc., Norwood, MA, 2006.

[13] Lattice ispMACH 4A CPLD Family Datasheet. Lattice Semiconductor Corporation, Hillsboro, OR, 2004.

[14] J. G. Graeme, G. E. Tobey, L. P. Huelsman. *Operational Amplifiers, Design and Applications*. McGraw-Hill Book Company, New York, 1971. ISBN 07-064917-0.

[15] National Semiconductor LMH6646 High-Speed, Rail-to-Rail Input and Output Amplifier Datasheet. National Semi, Santa Clara, CA, 2005.